Understanding and quantifying focused, indirect groundwater recharge from ephemeral streams using water table fluctuations

M. O. Cuthbert[1,2], R. I. Acworth[2], M. S. Andersen[2], J. R. Larsen[2,3,4], A. M. McCallum[2], G. C. Rau[2], and J. H. Tellam[1]

[1]School of Geography, Earth and Environmental Sciences, University of Birmingham, Birmingham, UK, [2]Connected Waters Initiative Research Centre, UNSW Australia, Sydney, New South Wales, Australia, [3]School of Geography, Planning, and Environmental Management, University of Queensland, Brisbane, Queensland, Australia, [4]Institute of Earth Surface Dynamics, University of Lausanne, Lausanne, Switzerland

Abstract Understanding and managing groundwater resources in drylands is a challenging task, but one that is globally important. The dominant process for dryland groundwater recharge is thought to be as focused, indirect recharge from ephemeral stream losses. However, there is a global paucity of data for understanding and quantifying this process and transferable techniques for quantifying groundwater recharge in such contexts are lacking. Here we develop a generalized conceptual model for understanding water table and groundwater head fluctuations due to recharge from episodic events within ephemeral streams. By accounting for the recession characteristics of a groundwater hydrograph, we present a simple but powerful new water table fluctuation approach to quantify focused, indirect recharge over both long term and event time scales. The technique is demonstrated using a new, and globally unparalleled, set of groundwater observations from an ephemeral stream catchment located in NSW, Australia. We find that, following episodic streamflow events down a predominantly dry channel system, groundwater head fluctuations are controlled by pressure redistribution operating at three time scales from vertical flow (days to weeks), transverse flow perpendicular to the stream (weeks to months), and longitudinal flow parallel to the stream (years to decades). In relative terms, indirect recharge decreases almost linearly away from the mountain front, both in discrete monitored events as well as in the long-term average. In absolute terms, the estimated indirect recharge varies from 80 to 30 mm/a with the main uncertainty in these values stemming from uncertainty in the catchment-scale hydraulic properties.

1. Introduction

Dryland regions (semiarid and arid regions but excluding hyperarid deserts) are expanding and now represent ~35% of the global landmass, support a population of around 2 billion people (90% of which live in developing countries), 50% of the world's livestock, 44% of all cultivated land and contain some of the most important wetlands in the world [*Hassan et al.*, 2005]. Water scarcity is becoming more critical in dryland areas due to population growth and urbanization, increasing irrigation demands, and climate change [*Scanlon et al.*, 2006; *Taylor et al.*, 2013]. In the wider Earth Science context, understanding groundwater recharge processes in drylands is also important for the interpretation of paleoclimatic proxy archives [*Cuthbert et al.*, 2014], and their longer-term sensitivity to change. Furthermore, understanding the relationships between climate and groundwater availability in drylands may enable us to understand better our own origins as human beings [*Cuthbert and Ashley*, 2014]. However, the understanding and quantification of groundwater recharge processes in dryland areas remains a major challenge worldwide [*Wheater et al.*, 2010].

In drylands, the climate has large atmospheric water demands and temperature contrasts, surface water flows are infrequent but potentially damaging and populations are sparse and often have limited economic resources [*Wheater et al.*, 2010]. Groundwater recharge in drylands predominantly occurs via leakage from ephemeral streams [*Simmers*, 1997, 2003]. Recharge can also occur more diffusely under the right conditions. For example, where sufficient preferential flow pathways exist to enable flow to by-pass otherwise dry soil profiles, or where soil moisture deficits are limited due to thin soils or lack of vegetation [*Cuthbert and*

Tindimugaya, 2010; *Cuthbert et al.*, 2013], or in Mediterranean climates with a winter rainy season when evapotranspirative losses are lower [*van Loon and van Lanen*, 2013]. However, these diffuse processes are, arguably, more widely understood and already successfully included in large-scale hydrological models, while the major areas of uncertainty exist in areas where recharge from surface water bodies such as ephemeral streams dominates [*Döll and Fiedler*, 2007; *Epstein et al.*, 2010; *Wheater et al.*, 2010]. Following *Healy* [2010], here we use the term "focused recharge" to refer to any recharge from a surface water body, and "indirect recharge" as a subtype of focused recharge whereby recharge occurs due to infiltration from streambeds such as the ephemeral streams that drain semiarid mountain front systems.

Systematic, multiyear observations of groundwater dynamics in ephemeral stream catchments are very rare and only reported for a few sites worldwide [*Besbes et al.*, 1978; *Carling et al.*, 2012; *Goodrich et al.*, 2004; *Pool*, 2005; *Shentsis and Rosenthal*, 2003]. Most dryland hydrological studies have been "top down," attempting to characterize groundwater recharge using a water balance approach based on surface measurements. Such methods are complicated by the inherent nonlinearities in predicting rainfall-runoff relationships, the difficulties of measuring flows and therefore transmission losses accurately in such environments, and transience in the nature of streambed losses [*Shanafield and Cook*, 2014]. Where transmission losses can be measured well or predicted, estimations of recharge are then hampered by the difficulty of estimating transpiration losses and/or lateral subsurface flow behavior due to alluvial structures [*Telvari et al.*, 1998]. Furthermore, upscaling from point-scale measurements to larger scales can be highly problematic [*McCallum et al.*, 2014].

In contrast, observations of the water table fluctuations of a catchment can provide the most direct measure possible of the recharge behavior, as they integrate the recharge response over a spatial footprint much larger than that of the measurement (borehole) scale. Estimating indirect recharge from time series of groundwater level measurements has been the subject of much research, but almost exclusively focused on inverse solutions of the transient mounding equations in various forms [*Abdulrazzak and Morel-Seytoux*, 1983; *Dillon and Liggett*, 1983; *Hantush*, 1967; *Moench and Kisiel*, 1970]. However, this previous work has not generally accounted for the background groundwater recession behavior or lateral boundary conditions. Furthermore, published studies are mostly based on data from a single piezometer or single event, therefore restricting its applicability. Finally, the available analytical approaches struggle with the complexity of the form of the input function for time varying recharge.

In this paper, we first develop a generalized conceptual model for understanding water table fluctuations in ephemeral stream catchments using insights gained from analytical and numerical models of idealized aquifers. By accounting for the recession characteristics of a groundwater hydrograph, we then present a simple but powerful new approach to quantifying indirect recharge separately over both the long term and on an event basis. This model is then tested using a unique monitoring database of groundwater dynamics from an ephemeral stream catchment in NSW, Australia.

2. Theoretical Background

2.1. The Water Table Fluctuation Method for Quantifying Recharge

The basis of the water table fluctuation (WTF) technique for quantifying recharge is the following equation:

$$R = S_y \frac{\partial h}{\partial t} + D \tag{1}$$

where R is the rate of recharge [$L\ T^{-1}$], S_y is specific yield, t is time [T], h is hydraulic head [L], and D is the rate of net groundwater drainage (or "rate of groundwater flux recession") [$L\ T^{-1}$] [*Cuthbert*, 2010]. This assumes that changes in groundwater level in an aquifer are controlled solely by the balance of recharge and net groundwater drainage away from a given observation point and ignores other factors such as entrapped air, barometric fluctuations, or local groundwater abstraction. The main limitations of the WTF method stem from difficulties of defining and estimating specific yield, and accounting for the drainage term (D) robustly [*Healy and Cook*, 2002].

2.2. The General Form of Water Table Fluctuations in Catchments Dominated by Indirect Episodic Recharge

An improved understanding and estimation of D has recently been proposed for the 1-D groundwater flow equations under uniform recharge [*Cuthbert*, 2010, 2014]. However, an adequate method for dealing with
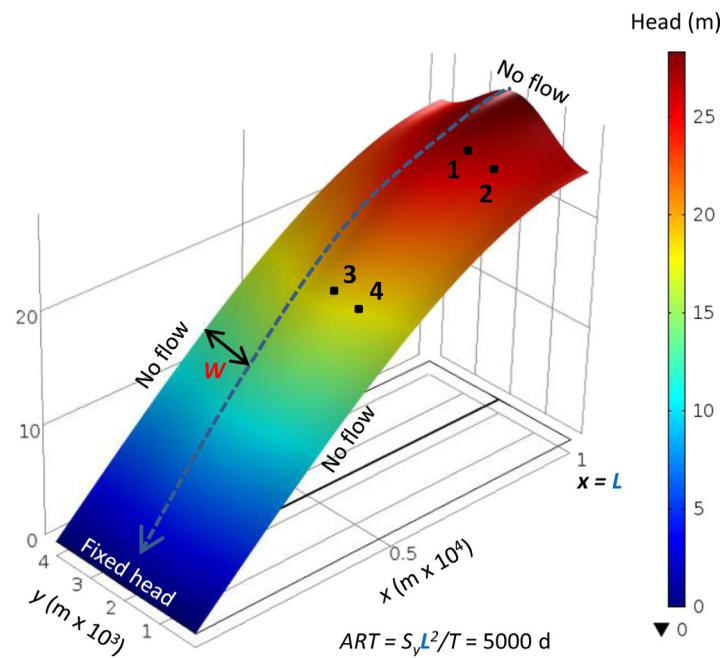
Figure 1. Model of an idealized aquifer receiving indirect recharge from an ephemeral stream. The parameters used were as follows: $T = 200$ m²/d, $S_y = 0.01$. Dashed blue arrow represents the stream recharge boundary. Heads are relative to the fixed head boundary at $x = 0$ and represent the water table during a streamflow/recharge event. Numbers 1–4 are locations that represent the computed groundwater hydrographs in Figure 2.

the recessional characteristics of a catchment in which recharge is dominated by losses from an ephemeral stream has not so far been proposed. It is therefore addressed here with regard to the idealized two-dimensional aquifer shown in Figure 1. It is bounded at one end (at $x = L$) by a no flow boundary—this may represent the edge of an alluvial aquifer abutting a mountain front, for example, typical in headwater ephemeral stream settings [*Pool*, 2005; *Simmers*, 1997]. The aquifer episodically receives surface runoff via a stream channel flowing in the x direction from higher elevations across this boundary which is then received by the aquifer beneath via streambed infiltration during episodic flow events. The downstream boundary condition at ($x = 0$) is a constant head boundary representing a typical discharge zone such as the transition to a perennial stream, wetland, or terminal lake. The lateral boundaries are no flow, thus the system is representative of a series of parallel ephemeral streams, again a reasonable simplification in a dryland setting. The linearized groundwater flow equation in two-dimensions for such an aquifer, here assumed to be homogeneous and isotropic, may be written as follows:

$$R = S_y \frac{\partial h}{\partial t} - T \left(\frac{\partial^2 h}{\partial x^2} + \frac{\partial^2 h}{\partial y^2} \right) \tag{2}$$

where T is transmissivity [$L^2\,T^{-1}$], and x and y are orthogonal length variables [L] as shown in Figure 1. This linearization assumes that the fluctuations in water table elevations are small compared with the saturated thickness of the aquifer.

For some time during and after an episodic streamflow event, we would expect a groundwater mound to rise and decay in the vicinity of the stream. Assuming that the recharge occurs along the length of the stream, it is effectively acting as a line source during the recharge period. We would thus expect the pressure wave generated to propagate transversely toward the lateral boundaries, at a distance W in the direction perpendicular to the stream, with an aquifer response time (ART), or time constant, of $t_{lat} = W^2 S_y/T$ [*Currell et al.*, 2014; *Domenico and Schwartz*, 1998; *Rousseau-Gueutin et al.*, 2013]. This aquifer event response will be superimposed on a longer-term background recession acting longitudinally in the direction parallel to the stream due to drainage to the perennial stream reach downstream, with a characteristic ART of $t_{long} = L^2 S_y/T$.

It is clear from a comparison of equations (1) and (2) that the groundwater flux recession rate, D, is given by:

$$D = -T \left(\frac{\partial^2 h}{\partial x^2} + \frac{\partial^2 h}{\partial y^2} \right) \tag{3}$$

The first and second terms on the RHS of equation (3) express the superposition of the longitudinal recession and the transverse recession, respectively.

To illustrate these concepts, the scenario described above and illustrated in Figure 1 has been modeled numerically using COMSOL Multiphysics (v5.1). The indirect recharge was simulated as an imposed flux
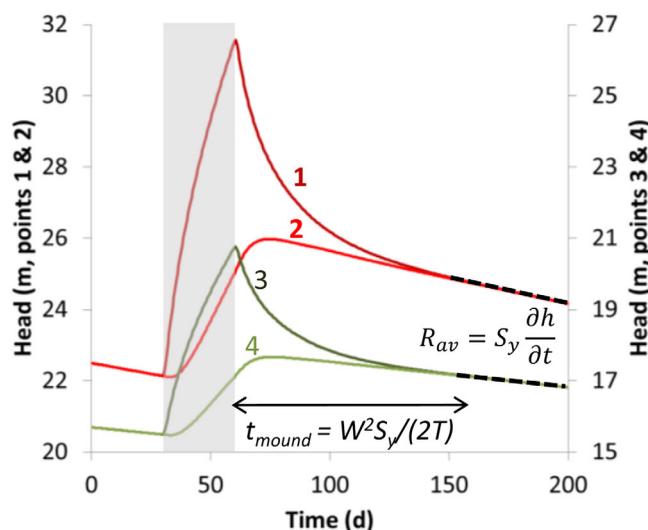
Figure 2. Output from the four locations in the model illustrated in Figure 1 showing superposition of transverse and longitudinal recessional characteristics. Grey shading indicates the period of steady flux input at the stream boundary. Black dashed lines show the exact proportionality between the variation of long-term (straight line) groundwater head recession down the catchment and the long-term recharge, i.e., the long-term recharge rate is equal to the specific yield multiplied by the long-term head recession rate.

boundary condition across a constant width of 20 m. This implicitly assumes that there is insignificant lateral spreading of the wetting front beneath the stream which is reasonable for cases where the depth to water table is less than the width of the channel [*Nimmo et al.*, 2002]. However, the applied recharge from the channel varied in space along the reach, with recharge decreasing linearly to zero between the upstream and downstream boundaries—an arbitrary distribution but one which mirrors the finding of previous research, that indirect recharge decreases away from runoff source areas such as mountain blocks [*Simmers*, 1997]. A long time series of identical episodic recharge events, each with a constant flux and duration, was modeled to bring the system to a quasi-steady state. The heads at points 1–4 were then output from the model for the last event and are shown as hydrographs in Figure 2. The parameters used are given in the legend for Figure 1.

Figure 2 shows how the background (longitudinal) recession is expressed as a straight line with a transverse mounding event superimposed upon it. The time scale for the decay of the mound can be estimated using an analytical solution. The analogous idealized problem of the 1-D redistribution of heads following a change in flux at one boundary (i.e., $y = 0$ at the stream), and a no-flow boundary at $y = W$ (i.e., an aquifer half space assuming parallel streams) is given by Bruggeman's equation 135.02 [*Bruggeman*, 1999]. Using this solution, it is possible to show that 99% of the transience created by a change in flux at the stream boundary will have decayed away within $t = t_{mound} \sim W^2 S_y/(2T)$ (i.e., half of $t_{lat.}$) since the change in flux. For the present case of the ideal aquifer, example plotted in Figure 2, $t_{mound} \sim 100$ days.

Furthermore, where recharge is distributed evenly across a catchment, recent theoretical work [*Cuthbert*, 2014] shows that straight line recession behavior is expected prior to $t_{lin} = x^2 S_y/(16T)$ since a recharge event occurred, where x is the distance from the monitoring point to the downstream fixed head boundary. In our modeled example, L is significantly greater than W, as you would expect in most natural settings, and thus t_{mound} is smaller than t_{lin} over much of the catchment. Hence, the straight line recession is observable under such conditions, as long as the time between recharge events is greater than t_{mound}. A further point worth noting here is that straight line recessions are also expected in contexts where flow lines are divergent [*Cuthbert*, 2014]. Thus, where an aquifer is bounded by streams that are not parallel, the mounding time scales may vary along the length of the streams, but the long-term recession would still be expected to be linear at early times following the cessation of recharge.

Straight line background recessions are observed in our synthetic example in line with the theory developed for evenly distributed recharge, despite the modeled recharge actually varying spatially. It is important to demonstrate that this feature of longitudinal recessions is a generally applicable one for the case of spatially variable recharge. Thus, additional analysis is needed as outlined in the next section.

2.3. Groundwater Flux Recession in Catchments With Spatially Variable Recharge
An expression for the recession of an ideal 1-D aquifer from an arbitrary initial condition is given by equation 10 of Venetis [*Venetis*, 1971]. In order to test the possible form of the longitudinal recession for the case considered above (i.e., recharge increasing linearly from zero at a downstream constant head boundary condition

($h = 0$) at $x = 0$ to R_{max} at $x = L$), it is useful to set the initial condition ($h_0(x)$) to the head distribution under steady state conditions. For $R = R_{max}x/L$, then it is straightforward to show that:

$$h_0(x) = -\frac{R_{max}x^3}{6LT} + \frac{R_{max}Lx}{2T}$$ (4)

Venetis [1971, equation 10] gives the following expression for the variation in head as:

$$h(x, t) = \frac{1}{L}\sum_{n=1, \ 3, \ 5...} e^{\frac{-n^2\pi^2Tt}{4SL^2}} sin\left(\frac{n\pi x}{2L}\right) \int_0^{2L} h_o sin\left(\frac{n\pi x}{2L}\right) dx$$ (5)

From this equation, the conditions under which spatially variable recharge should produce straight line recessions can be analyzed. Since we are only considering 1-D (longitudinal) flow in this case, (i.e., just considering the recession which occurs after any mounding due to indirect recharge, and variation in head in the y direction, has dissipated), the net groundwater drainage can be simplified to:

$$D = -T\frac{d^2h}{dx^2}$$ (6)

Equations (4)–(6) have been used to plot Figure 3 with D normalized to the recharge value at the midpoint of the model domain ($x/L = 0.5$). This shows how the modeled groundwater flux recession rate varies following a recharge event relative to the initial recharge rate across a range of ARTs. Values close to 1 on the vertical axis thus indicate that the recession is a straight line and accurately predicts the spatially varying recharge rate.

This shows that for some time following cessation of recharge, the straight line recessions are a direct indicator of the variation of the spatial variability in long-term recharge. Furthermore, this analysis indicates that even for this case of spatially varying recharge, $t < t_{lin}$ [*Cuthbert*, 2014] can provide a reasonable (and conservative) measure of the length of time straight line recessions can be expected to last.

2.4. A Water Table Fluctuation Method for Quantifying Indirect Recharge
Based on the preceding theory, we can now propose a new WTF approach to estimate episodic indirect recharge. As with any WTF recharge estimation methodology, it should only be used if a robust conceptual model warrants it. Thus, as per the methodology outlined by [*Cuthbert*, 2010] for estimating diffuse recharge using WTFs, the first step to be taken should be delineating the main hydrogeological boundaries, considering the likely controls on recharge due to the presence of superficial deposits and the climatic context, and utilizing estimations of aquifer properties where possible. Furthermore, the time series of groundwater level data to be used must be of sufficient temporal resolution, representative of the local water table position, and sufficiently distant from the influence of pumping wells.

The analytical and numerical models of an idealized catchment described above suggest that where a straight line groundwater level recession is observable, it can be used in two ways to estimate indirect groundwater recharge:

Figure 3. Rates of groundwater flux recession (D) after recharge ceases normalized to the recharge rate (R) used to determine the initial conditions, for variations in aquifer response time (ART = S_yL^2/T) and time, for a groundwater monitoring point positioned at $x = 0.5\ L$. Shaded zone is for $t < t_{lin}$ as defined by *Cuthbert* [2014].

1. The slope of the straight line recession can be used to estimate the "long-term" ratio of R/S_y (or the actual recharge if S_y is known) by the following equation:
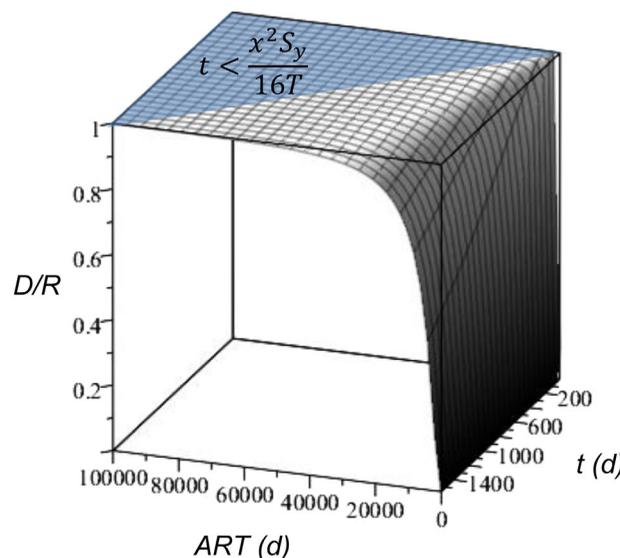
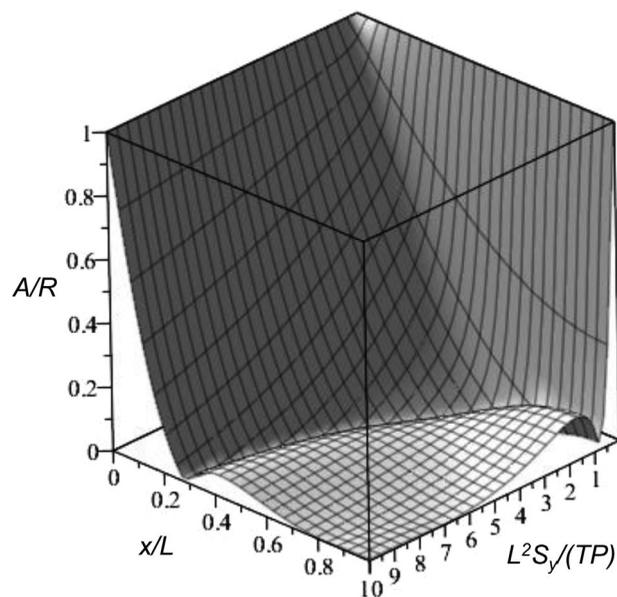$$R_{av} = S_y \frac{\partial h}{\partial t} \qquad (7)$$

Figure 4. Variation in the amplitude of the flux recession rate (A) normalized to the average recharge rate (R) plotted against the ratio of the ART ($L^2 S_y/T$) to the period of recharge variation (P) and the position of the groundwater monitoring point with respect to the catchment boundaries (x/L). Plot created using equation (8) from *Cuthbert* [2010]. Away from the fixed head boundary, ART/P must be less than 1 for A/R to deviate significantly (more than 10%) from zero, i.e., variations in recharge at periods less than the ART will be damped out and not expressed as variations in the flux recession rate.

Since the antecedent history of the system is not necessarily known, the meaning of "long term" cannot always be precisely determined. However, as Figure 4 indicates, away from the fixed head boundary, the aquifer damps out variations in recharge so that significant variations in flux recession rate only occur due to recharge variations with periods greater than the ART. Hence, away from a fixed head boundary, observation of a straight line recession and use of equation (7) will provide an estimate of the recharge occurring over the previous time period defined by the ART (Figure 4).

2. On an event basis, the background recession can be added to a groundwater hydrograph time series to reveal the change in head due exclusively to event recharge from the stream. This is illustrated in Figure 5, where the effect of the long-term recession rates has been removed in this way from the groundwater hydrographs already shown in Figure 2. If the system is behaving in the manner expected by the conceptual model outlined, for $t > t_{mound}$, the result should be a step change in head (Δh) where:

$$R_{event} = S_y \Delta h \qquad (8)$$

Figure 5 indicates that, with the longitudinal recession removed, significant head increases still occur nearer to the stream due to the transverse spreading of the pressure wave generated by the flow event (hydrographs 1 and 3). However, further away from the stream (hydrographs 2 and 4), this effect becomes almost unnoticeable, with the response now resembling a gradual step change in head.

Both techniques ultimately rely on knowing the value of S_y for estimating actual recharge and this can be challenging to obtain at the right spatial scale. However, S_y can be estimated from the definition of t_{mound} ($W^2 S_y/(2T)$) if t_{mound} is determined by observation, T is estimated, for example, from a pumping test, and W from the geometry of the system.

3. A Case Study From Middle Creek, NSW, Australia

3.1. Catchment Context

The catchment has been described in detail previously [*Andersen and Acworth*, 2009; *Rau et al.*, 2010] and is only briefly summarized here. Middle Creek (via Horsearm Creek) is an ephemeral tributary to Maules Creek, itself a tributary to the Namoi River in the headwaters of the Murray Darling Basin, NSW, Australia (Figure 6). The Nandewar Range (part of the Great Dividing Range) to the north-east receives approximately 1100 mm/a of precipitation in the long term. Rainfall is generally well distributed throughout the year; however, the rainfall intensity varies substantially with heavy rains generally occurring in the summer months (December–February). The rainfall is also influenced by longer-term fluctuations in the El Niño Southern Oscillation Index (ENSO), with higher than average rainfalls in the positive phase (La Niña) and lower than average rainfalls in the negative phase (El Niño).
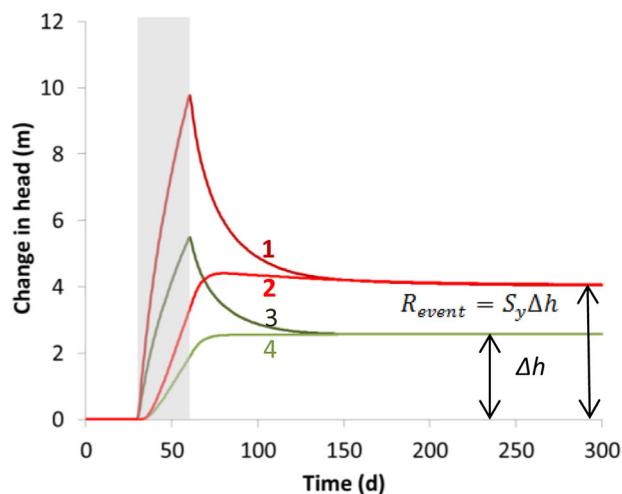
Figure 5. Groundwater hydrographs for the cases shown in Figure 2 with the long-term recession removed to reveal the effects solely due to recharge from the stream. Grey shading indicates the period of steady flux input at the stream boundary.

Large storm events generate runoff from the steep headwaters of the Middle Creek catchment which is comprised of Miocene volcanic rocks overlain by thin soils with forested land use. Flow is delivered across the mountain front (defined by a thrust fault) and onto a moderate gradient (1–2%), Quaternary age, alluvial fan up to 40 m thick. This overlies Permian sedimentary deposits (claystones, siltstones, sandstones, conglomerates, and coal measures) and Carboniferous crystalline rocks, metasediments, and volcanic deposits. The degree of hydraulic connectivity between the Quaternary alluvium and these underlying formations is presently unknown. As can be seen in Figure 6, the land downstream of the mountain front is largely cleared for grazing, except for a narrow vegetated zone adjacent to the creek. A well-delineated ephemeral channel has cut through clay-rich soils which otherwise blanket the alluvium. The main channel is typical of an episodic high energy stream comprising sand and gravel deposits often forming pool-riffle sequences and cobble to boulder size lag. Ephemeral flows have been observed to extend all the way to the confluence with Horsearm Creek and Maules Creek. Rainfall on the alluvial fan itself decreases to the southwest away from the Nandewar Range. At Middle Creek Farm, the recent record indicated 522 mm/a for 2014, Bellevue farm situated further downstream averaged 534 mm/a, and both are in contrast to the 912 mm/a for Mount Kaputar in the catchment headwaters (see Figure 6 for locations).

For the time series available, Middle Creek flows when the cumulative rainfall in the month prior exceeds around 140 mm and the majority of runoff is assumed to be generated in the steep and low-permeability mountain headwaters. The regional hydraulic gradient indicated by available groundwater level data is approximately northeast to southwest. There is little groundwater pumping in the Middle Creek area itself. However, Middle Creek is just one of a series of ephemeral streams draining into Maules Creek and providing recharge to aquifers which are extensively pumped for cotton irrigation in the Namoi Valley downstream.

3.2. Monitoring Installations and Testing Methods

Six 0.168 m diameter boreholes (Figure 6) were drilled in 2012 using an air flush rotary/hammer method with advancing steel casing and installed with either two or four multilevel piezometers, each screen being hydraulically isolated using bentonite seals. After completion, the piezometers were developed by air lifting using a compressor. Care was taken not to blow air into the screened section of the piezometers. Air lifting was continued until the discharged water was clear. Details of the resulting 20 piezometers are given in the supporting information. The drill cuttings revealed that the alluvium comprises a highly heterogeneous layered system of mixed gravel, sand, clay, and silt. The large variation in grain size is as expected given the alluvial fan depositional setting.

Every piezometer was monitored at 15 min frequency using Solinst Levelloggers, compensated using a barometric logger situated in a borehole at East Lynne (BH20) which recorded air pressure at exactly the same times. This was hung in the piezometer at approximately 2 mbgl to avoid large temperature variations and thereby minimize any diel artifacts in the pressure data [*Acworth et al.*, 2014], while remaining above the water column. Manual dip-tape measurements were made each time the data were downloaded and used to check that no significant drift in the loggers was occurring. These measurements were also used, in combination with elevation data of each borehole datum measured using a Differential GPS, to convert the data to hydraulic head with respect to Australian Height Datum (AHD).

A constant rate pumping test was carried out at Elfin Crossing (BH14, Figure 6) and analyzed using a transient model. For this analysis, the Theis [*Theis*, 1935] equation was used incorporating the superposition of an injection
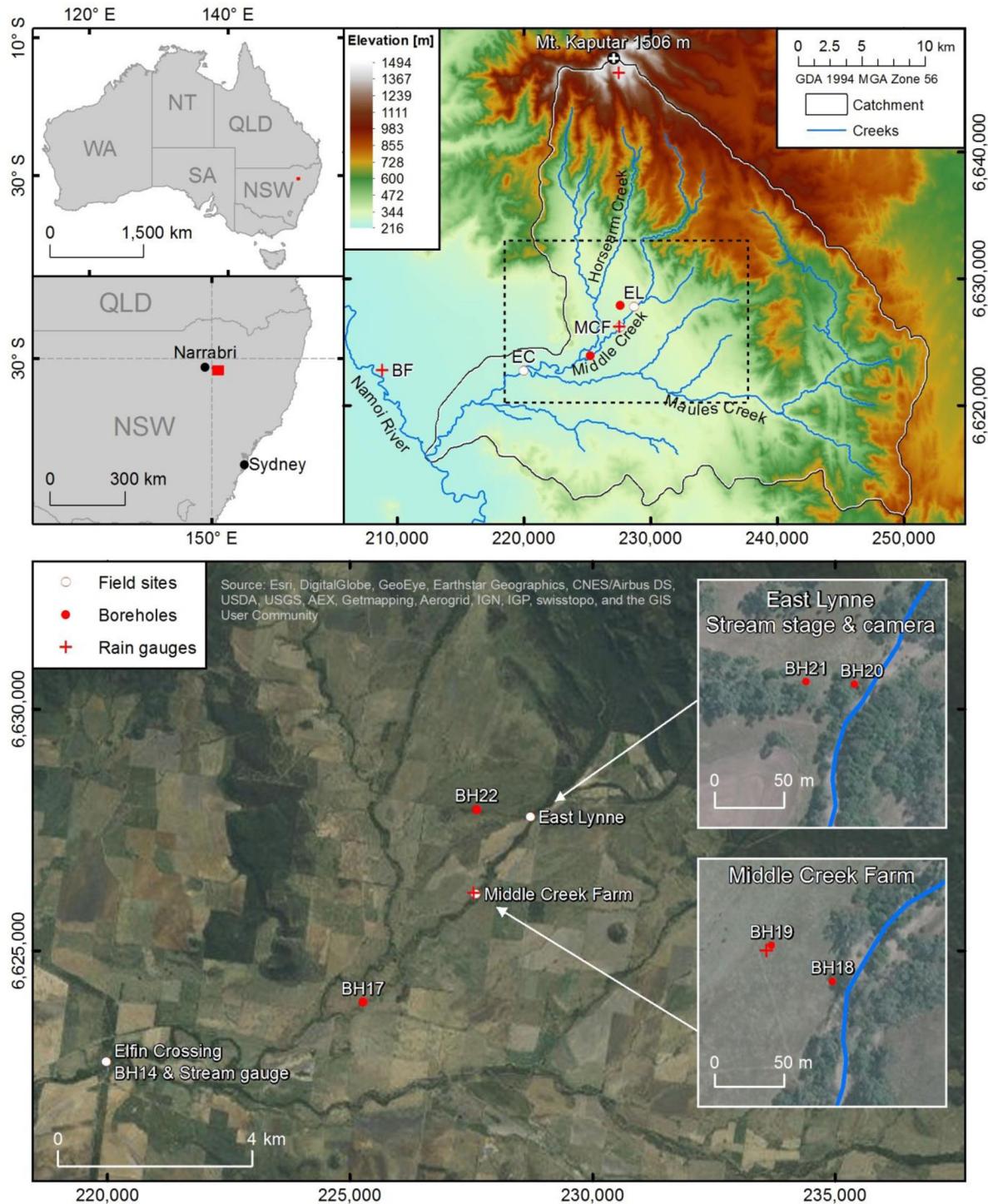
Figure 6. Middle Creek and monitoring installations in the context of the Maules Creek catchment. DEM used courtesy of Geoscience Australia. BF = Bellevue Farm; EC = Elfin Crossing; MCF = Middle Creek Farm; EL = East Lynne.

image well to implement a recharge boundary due to the close proximity of the perennial section of Maules Creek (~35 m). The drawdown data were fitted to the model by varying the hydraulic parameters (T, S) in order to minimize the RMSE. Details of the pumping test and analysis can be found in the supporting information.

Stream stage was measured adjacent to Boreholes BH20-BH21 at East Lynne using a Campbell Scientific CS450 pressure transducer logged by a Campbell Scientific CR1000 since June 2013. Since June 2012, a digital camera
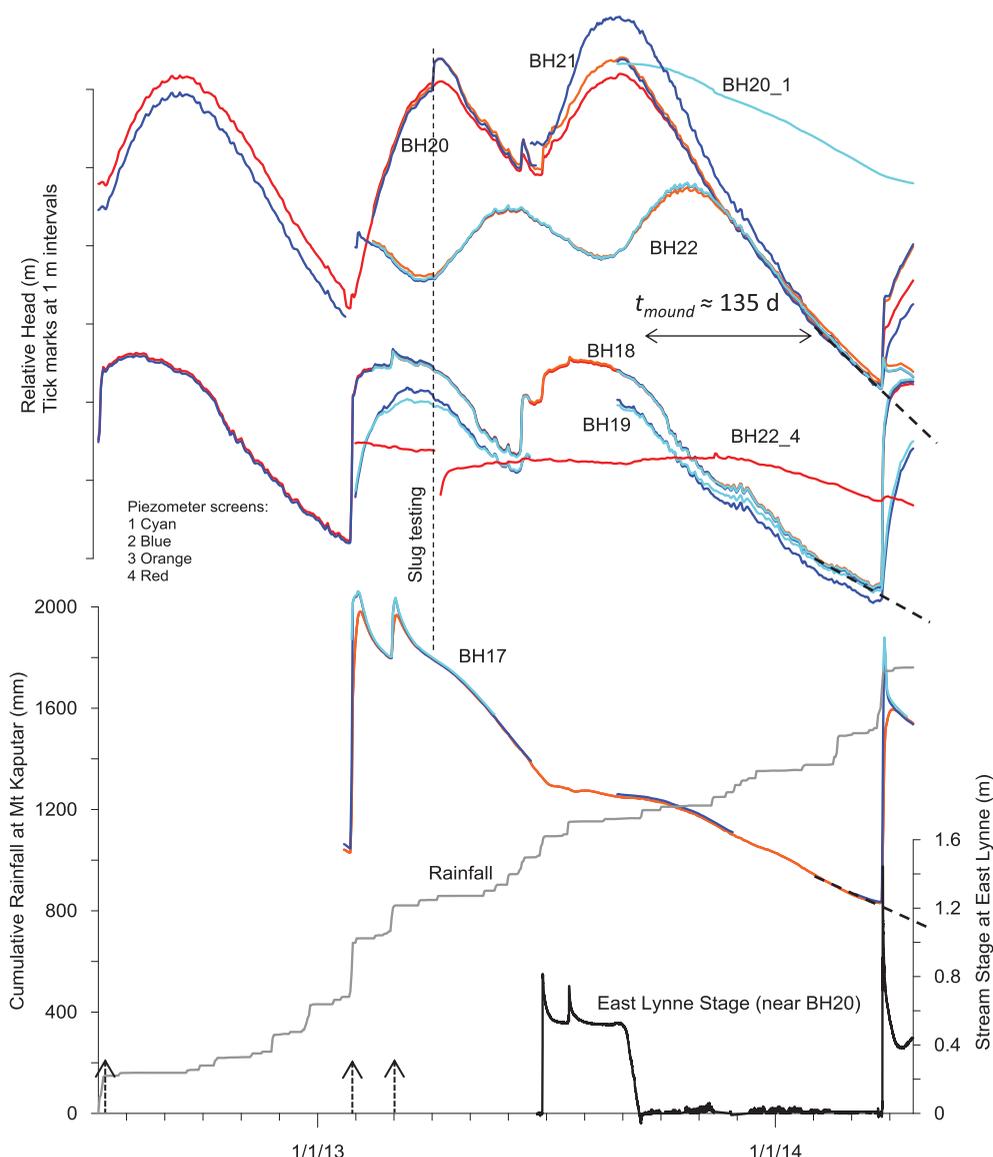
Figure 7. Groundwater hydrographs (daily average), stream stage, and cumulative rainfall. Heads are given on the same vertical scale, but with the absolute values shifted to enable the hydrographs to be compared. Dashed black arrows indicate streamflow events at East Lynne (BH20-21) captured by an automatic camera, prior to the installation of stream stage monitoring. Bold dashed black lines indicate periods of straight line groundwater recession. The different piezometer screens for each borehole are colored according to the key shown with 1–4 being shallow to deep, respectively. The time of slug testing is also marked as it led to a temporary disturbance of the natural heads.

placed at East Lynne has been capturing a record of flows in the creek which can also be used to determine the timing and approximate magnitude of the flow events. It is noted that some small but greater than zero stage measurements are apparent between September 2013 and March 2014 in the East Lynne stage hydrograph (Figure 7) caused by temperature-driven air pressure differences between the transducer in the creek and the hut on the creek-bank in which the data logger was housed. However, based on site visits and photographic evidence from the automated on-site camera, there was no flow in the creek during this period.

A full Campbell Scientific weather station was installed next to BH19 at Middle Creek Farm and has been recording since August 2013.

3.3. Groundwater Hydrograph Dynamics

Time series of heads recorded in every piezometer are shown in Figure 7 alongside the stream hydrograph at BH20 (East Lynne) and the cumulative rainfall record from Mount Kaputar. We consider this to be a

globally unparalleled data set with respect to the intensity of groundwater level data being collected in an ephemeral stream catchment, allowing an unprecedented insight into its hydrodynamics. More detailed additional plots for nearby groups of piezometers are given in the supporting information Figure S1. Heads varied between 3 and 8 m below ground level with greatest unsaturated zone thickness occurring beneath the streambed at the most upstream location (BH20 and BH21), and the greatest total unsaturated zone thickness occurring at the top end of the reach, furthest away from ephemeral streams (BH22). There is evidence of barometric fluctuations seen in piezometers from BH18-20, but not in BH17. This suggests the presence of materials with low permeability above the screened depth in the BH18-20 piezometers [*Acworth et al.*, 2014]. Loading responses also occur at times of episodic surface flows as indicated by sudden increases in head seen in the groundwater hydrographs, corresponding with sudden stream stage increases in Middle Creek. This is consistent with the variable lithology encountered during drilling, and the variability in formation hydraulic conductivity implied by drawdowns observed during hydrochemical sampling. However, in general, the groundwater fluctuations are dominated by increases coincident with streamflow events in Middle Creek followed by recessions. The exceptions are BH20_1 and BH22_4 which are clearly screened within low-permeability units and therefore show very slow responses in comparison to the other piezometers. Following an ephemeral flow event, groundwater head changes are characterized by a rapid increase in gradients between piezometers followed by a more gradual reequilibration occurring on three distinct length and time scales of hydraulic head redistribution. These can be interpreted as being due to vertical, transverse, and longitudinal propagation of the pressure increase induced by streamflow losses to the underlying alluvium. Vertical downward hydraulic gradients are initially induced near the creek which then dissipate on the time scale of days to weeks (for example, compare BH17_1 and BH17_4 in Figure 7). Transverse gradients away from the creek dissipate on the time scale of weeks to months, and longitudinal, down-catchment, gradients are apparent throughout the whole monitoring period suggesting they persist over longer time scales of years.

Consistent with the idealized groundwater hydrograph responses to episodic indirect recharge described in section 2 (Figures 1 and 2), there is an observed time lag and amplitude attenuation with distance away from Middle Creek which is particularly pronounced at the most distant location from Middle Creek, BH22. Also akin to the idealized hydrographs is the mounding which occurs after a streamflow event, followed by a gradual transition to a straight line recession during extended periods of no streamflow. In this case, t_{mound} estimated as the time between the cessation of surface flow in the creek and the return to conditions of straight line groundwater recession is approximately 135 days. Thus, the straight line recession is only seen once in the time series (February–March 2014) when the time between streamflow events exceeds this time scale. As shown by the dashed black lines in Figure 7, the steepness of these long-term recessions decreases with distance downstream. For BH20, BH21, and BH22, located a similar distance from the mountain front, but different distances from Middle Creek (2, 37, and 1111 m, respectively), the mounding behavior is initially different for each borehole. However, at later times, the recession converges to a remarkably consistent straight line gradient, as expected from the theoretical considerations discussed above.

It is noted that during streamflow events, the head in BH21 rises to a slightly lower absolute level than the head at BH20, and there is flow away from the creek for the duration of the flow event, consistent with our conceptual model. However, the recession at BH21 is larger than that of BH20 which we believe is due to pumping from a nearby stock watering well located around 60 m west of BH21. It is a very minor abstraction (intermittent, wind-mill-driven pump and the numbers of livestock observed in the vicinity are low) although it nevertheless appears to produce a local cone of depression which influences the variation in water level at BH21. This is discussed further in section 3.4 in terms of its implications for the estimation of recharge. We also note that groundwater use by riparian vegetation remains unknown at this site. However, such water use is certain to contain a significant soil moisture component, especially during and following recharge events. Any impacts on the water table by direct groundwater use are therefore likely to be very small relative to the broader trends observed.

Small vertical head gradients, developed in response to streamflow events, are observed in the logger data at some locations and these differences are consistent with manual dip-tape measurements, thus not being artifacts of the logged time series. For BH17 and BH20 immediately adjacent to the stream, downward gradients occur after surface water flow events, consistent with the indirect recharge mechanism proposed, which then dissipate quickly over time since the event. In contrast at BH19, situated 50 m away from the stream, the
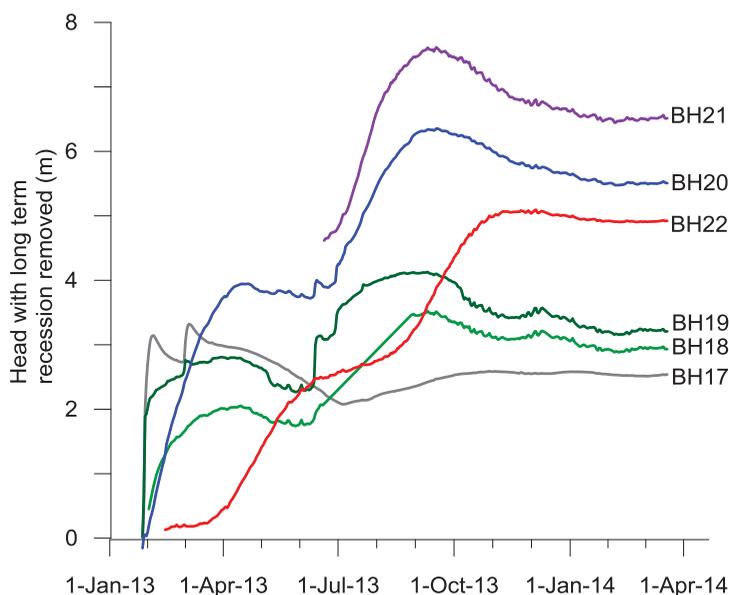
Figure 8. Groundwater hydrographs with background recessions "removed." The final head value represents the increase due to recharge from ephemeral streamflow since January 2013. Where continuous data were not available from data loggers (i.e., BH22, BH19, and BH21), the residual heads were calculated using dip-tape measurements taken just prior to the streamflow event in late January 2013.

gradient is upward following streamflow events. This is suggestive of water propagating through a more permeable layer at depth while equilibrating vertically as the recharge pulse dissipates transversely. Since the small vertical gradients equilibrate on a time scale much shorter than the transverse head gradients, it is a reasonable assumption that the groundwater level observations are mostly representative of the water table dynamics during the transverse and longitudinal recession periods. Thus, it is reasonable to apply the methodology proposed in section 2 which was based on a 2-D representation of an idealized aquifer which assumes no vertical flow is occurring.

3.4. Quantifying Recharge Using the New Methodology

The long-term straight line recessions were calculated using the data shown in Figure 7. A complication in this task was that each borehole hydrograph has a varying degree of barometric "noise" in the water level signal. Thus, a purely statistical approach, for example, using a cutoff for a particular coefficient of determination on a linear regression, was not deemed appropriate. Our approach was, therefore, to identify the time period from which the hydrographs at different distances from the creek converged onto a consistent linear recession after a streamflow event and until the groundwater levels began to respond to the next streamflow event. Since this is somewhat subjective, two reasonable end-member times were selected for start of the linear recession period, in this instance, 2 weeks apart from each other, in order to account for the subjective uncertainty (further apart than this and the mismatch becomes obvious). The recession rates were then calculated by averaging the incremental changes in head during the assigned periods. These two recession rates were then "removed" from the head time series by adding the calculated values, and the average residual heads have been plotted in Figure 8. The event-based estimates of R/S_y summed over 2013 were then calcu-

lated from Figure 8 and plotted against the long-term estimates in Figure 9, with error bars added to indicate the uncertainty in the analysis due to the variation in the chosen recession rate. A summary of these values and their uncertainties is given in Table 1.
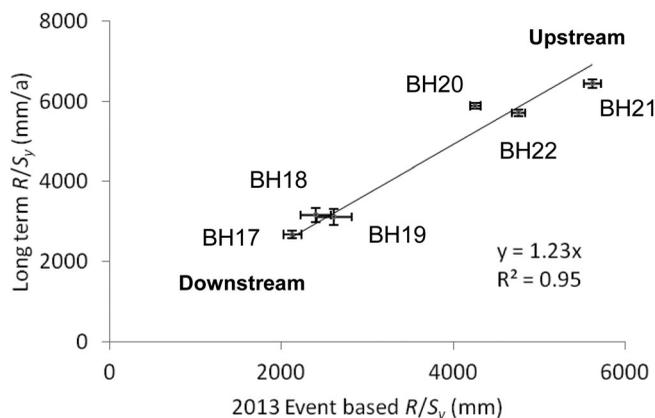
It is noted that the residual head increase at BH21 is larger than that at nearby BH20, probably due to the minor nearby abstraction as discussed in section 3.3. However, the long-term recession from BH21 eventually begins to converge with those of BH20 and BH22 suggesting that the effect is a transient one which diminishes during dry

Figure 9. Comparison of long-term and event-based indirect recharge estimates.

Table 1. Summary of Recession Rates and Recharge Estimates—All Values in mm/a

	Recession Rate	Residual Head Increase for 2013	Error in Estimated Value of R/S_y	Long-Term Recharge	Recharge in 2013	Error in Recharge
BH17	2678	2123	104	32	25	5.9
BH18	3118	2609	154	37	31	7.3
BH19	3166	2398	175	38	29	6.7
BH20	5711	4757	75	69	57	13.2
BH21	6444	5618	96	77	67	15.6
BH22	5892	4258	64	71	51	11.8

periods. Hence, although the derived R/S_y values for BH21 are likely to be overestimates they are still within the error bounds for BH20 and BH22.

In order to convert the estimates of R/S_y presented above into actual recharge, S_y must first be estimated. A best fit ($R^2 = 0.99$) value for T from the pumping test on BH14 was 115 m^2/d (see supporting information). From Figure 7, the mounding time scale at East Lynne can be estimated as the time from the cessation of flow in the stream until the convergence of the recessions onto a straight line, which is 135 days with an uncertainty of ±7 days as previously assigned to account for the uncertainty in the choice of the start of the straight line recession period. The half-space, W, can be estimated by halving the average distance from Middle Creek to the adjacent ephemeral creeks. Since there is some convergence of the adjacent creeks, and therefore variation in W, with longitudinal distance downstream from the mountain front (Figure 6), this calculation was only done for the East Lynne location where the adjacent streams are close to being parallel. Allowing for some uncertainty due to the slight convergence in the streams we estimate W to be 1.6 ± 0.1 km. Using the expression for t_{mound} given in Figure 2, this implies that the diffusivity (T/S_y) is ~9500 ± 700 m^2/d. Taking the pumping test value for T (115 ± 12 m^2/d) yields a value of S_y of 0.012 ± 0.003. This is reasonable given the prevalence of interbedded clay layers and also a significant proportion of fines within many layers of the alluvial material encountered in the catchment. Since a stage hydrograph was only available at East Lynne, t_{mound} could only be estimated for this location, but the resulting S_y value was applied to all piezometers. A summary of the recharge estimates and their uncertainties is given in Table 1.

What is immediately apparent is that, assuming S_y is not varying significantly within the catchment, the amount of groundwater recharge is generally decreasing with increasing distance from the mountain front. Furthermore, this trend is consistent between the long-term and event-based estimates suggesting that this is a persist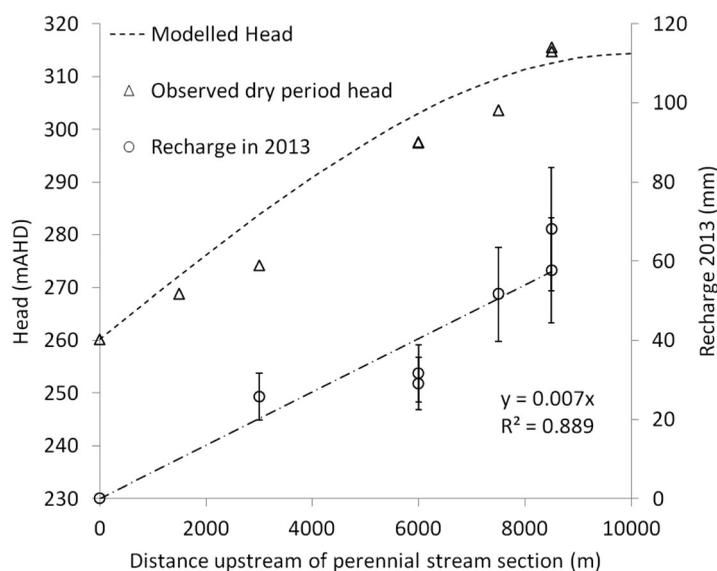ent feature of the recharge behavior in the catchment. Groundwater recharge for 2013 was lower than the estimated long-term average by around 23% (Figure 9). The long-term average value is representative of recharge occurring over the preceding period given by the ART which, using the above values for the catchment hydraulic diffusivity and a length of 10 km, is approximately 30 years. Using the estimate for S_y of 1.2% enables us to estimate the long-term (30 year) recharge in the catchment using this technique as over 70 mm/a close to the mountain front (BH20-22) and around 30 mm/a by 6 km further downstream. Similarly, indirect recharge for 2013 has been

Figure 10. Variation of estimated recharge with distance upstream and comparison of observed dry period heads (i.e., during a straight line recession period) with heads predicted using equation (4).

calculated and plotted against distance from the perennial downstream boundary indicating an almost linear relationship (Figure 10). The zero recharge point is defined as the most upstream perennial section of Horsearm Creek, 2 km upstream of Elfin Crossing. As a reality check for this system, since the change of recharge with longitudinal distance along the stream appears to be approximately linear, we have applied equation (4) with $R_{max} = 68$ mm/a, the maximum estimated for 2013, $T = 115$ m^2/d and $L = 10,000$ m. The computed and observed heads during a recession period in 2013 are plotted in Figure 10. The comparison is good given the simplicity of the model, and demonstrates further consistency between the derived recharge values, estimated aquifer parameters and the groundwater observations. While we acknowledge the uncertainty in the absolute magnitude in the recharge estimations, this highly heterogeneous alluvial system is a very challenging one in which to estimate hydraulic properties at the appropriate scale and in more homogeneous aquifers, the estimation of T or S_y should be even more straightforward.

3.5. Deviations Between Real and Ideal Catchment Behavior

Although the methodology we have presented is potentially very powerful, as with most analytical methods, several issues arise when applying them to field conditions. For instance, the model assumes parallel adjacent ephemeral channels but the field example includes adjacent channels that converge within the study reach. As noted, such deviation in the geometry will affect the accuracy of the t_{mound} estimations for calculating hydraulic parameters. However, straight line recessions are theoretically predicted [*Cuthbert*, 2014], and actually observable in catchments with nonuniform flow fields during long-term recession periods as in this field example. Hence such geometries do not affect the fundamental principle of deriving estimates of the R/S_y ratio by the method we have proposed. Other deviations of field situations from the analytical model are also possible such as differing drainage areas and streamflow timings for adjacent channels, lack of adjacent channels, and nonparallel impermeable boundaries at differing distances. These should be considered on a case by case basis, and where significant deviations are found, modifications to the methodology may be necessary to ensure accurate results.

4. Conclusions

We have developed a generalized conceptual model for understanding water table and groundwater head fluctuations in ephemeral stream catchments and, by accounting for the recession characteristics of a groundwater hydrograph, presented a simple but powerful new approach to quantifying indirect recharge both in the long term and on an event basis. Furthermore, a new, and globally unparalleled, data set of groundwater dynamics in a dryland ephemeral stream catchment from Middle Creek, NSW, Australia, has been used to test the theoretical ideas developed using idealized models.

From examination of the extensive field data set, we find that head responses to ephemeral streamflow events are controlled by pressure redistribution operating at three time scales from vertical flow (days to weeks), transverse flow perpendicular to the stream (weeks to months), and longitudinal flow parallel to the stream (years to decades). From application of the new methods to the field data set, we find that, in relative terms, groundwater recharge decreases linearly away from the mountain front to the perennial stream section and has a similar spatial pattern both in the recent events analyzed as well as over the longer term. In absolute terms, the long-term indirect recharge estimates vary from approximately 30 to 80 mm/a with the main uncertainty in these values stemming from the challenge of being able to estimate hydraulic properties at the appropriate spatial scale.

Further work will focus on the transferability of this approach to other dryland catchments which have sufficient groundwater level data available. While we noted in the introduction that multiyear observations of groundwater dynamics in ephemeral stream catchments are relatively rare, several data sets appear to show similar features to the data we have presented here [*Besbes et al.*, 1978; *Carling et al.*, 2012; *Goodrich et al.*, 2004; *Hoffmann et al.*, 2007; *Houston*, 2002]. Thus, we expect that this methodology will be directly applicable to other catchments. As longer time series become available from the Middle Creek catchment and others that have recently been established in similar environments, for example, as part of the NCRIS groundwater infrastructure in Australia, the approach will be an important tool to explore the relationship between groundwater recharge and climate change.

References

Abdulrazzak, M. J., and H. J. Morel-Seytoux (1983), Recharge from an ephemeral stream following wetting front arrival to water table, *Water Resour. Res.*, *19*(1), 194–200.

Acworth, R., G. C. Rau, A. M. McCallum, M. S. Andersen, and M. O. Cuthbert (2014), Understanding connected surface-water/groundwater systems using Fourier analysis of daily and sub-daily head fluctuations, *Hydrogeol. J.*, *23*(1), 143–159.

Andersen, M. S., and R. Acworth (2009), Stream-aquifer interactions in the Maules Creek catchment, Namoi Valley, New South Wales, Australia, *Hydrogeol. J.*, *17*(8), 2005–2021.

Besbes, M., J. Delhomme, and G. De Marsily (1978), Estimating recharge from ephemeral streams in arid regions: A case study at Kairouan, Tunisia, *Water Resour. Res.*, *14*(2), 281–290.

Bruggeman, G. (1999), *Analytical Solutions of Geohydrological Problems*, Elsevier, Amsterdam, Netherlands.

Carling, G. T., A. L. Mayo, D. Tingey, and J. Bruthans (2012), Mechanisms, timing, and rates of arid region mountain front recharge, *J. Hydrol.*, *428*, 15–31.

Currell, M., T. Gleeson, and P. Dahlhaus (2014), A new assessment framework for transience in hydrogeological systems, *Groundwater*, *54*, 4–14.

Cuthbert, M. (2010), An improved time series approach for estimating groundwater recharge from groundwater level fluctuations, *Water Resour. Res.*, *46*, W09515, doi:10.1029/2009WR008572.

Cuthbert, M. (2014), Straight thinking about groundwater recession, *Water Resour. Res.*, *50*, 2407–2424, doi:10.1002/2013WR014060.

Cuthbert, M., and G. Ashley (2014), A spring forward for hominin evolution in East Africa, *PloS one*, *9*(9), e107358.

Cuthbert, M., and C. Tindimugaya (2010), The importance of preferential flow in controlling groundwater recharge in tropical Africa and implications for modelling the impact of climate change on groundwater resources, *J. Water Clim. Change*, *1*(4), 234–245.

Cuthbert, M., R. Mackay, and J. Nimmo (2013), Linking soil moisture balance and source-responsive models to estimate diffuse and preferential components of groundwater, *Hydrol. Earth Syst. Sci.*, *17*(3), 1003–1019.

Cuthbert, M., A. Baker, C. N. Jex, P. W. Graham, P. C. Treble, M. S. Andersen, and R. Ian Acworth (2014), Drip water isotopes in semi-arid karst: Implications for speleothem paleoclimatology, *Earth Planet. Sci. Lett.*, *395*, 194–204.

Dillon, P., and J. Liggett (1983), An ephemeral stream-aquifer interaction model, *Water Resour. Res.*, *19*(3), 621–626.

Döll, P., and K. Fiedler (2007), Global-scale modeling of groundwater recharge, *Hydrol. Earth Syst. Sci. Discuss.*, *12*(3), 863–885.

Domenico, P. A., and F. W. Schwartz (1998), *Physical and Chemical Hydrogeology*, John Wiley, N. Y.

Epstein, B., G. Pohll, J. Huntington, and R. Carroll (2010), Development and uncertainty analysis of an empirical recharge prediction model for Nevada's desert basins, *J. Nev. Water Resour. Assoc.*, *5*(1), 1–22.

Goodrich, D. C., D. G. Williams, C. L. Unkrich, J. F. Hogan, R. L. Scott, K. R. Hultine, D. Pool, A. L. Goes, and S. Miller (2004), Comparison of methods to estimate ephemeral channel recharge, Walnut Gulch, San Pedro River basin, Arizona, in *Groundwater Recharge in a Desert Environment: The Southwestern United States*, pp. 77–99, AGU, Washington, D. C.

Hantush, M. S. (1967), Growth and decay of groundwater-mounds in response to uniform percolation, *Water Resour. Res.*, *3*(1), 227–234.

Hassan, R. M., R. Scholes, and N. Ash (2005), *Ecosystems and Human Well-Being: Current State and Trends: Findings of the Condition and Trends Working Group*, Island Press, Wash.

Healy, R. W. (2010), *Estimating Groundwater Recharge*, Cambridge Univ. Press, Cambridge, U. K.

Healy, R. W., and P. G. Cook (2002), Using groundwater levels to estimate recharge, *Hydrogeol. J.*, *10*(1), 91–109.

Hoffmann, J. P., K. W. Blasch, D. R. Pool, M. A. Bailey, and J. B. Callegary (2007), Estimated infiltration, percolation, and recharge rates at the Rillito Creek focused recharge investigation site, Pima County, Arizona, in *Ground-Water Recharge in the Arid and Semiarid Southwestern United States*, *U.S. Geol. Surv. Prof. Pap.*, *1703-H*, pp. 185–220.

Houston, J. (2002), Groundwater recharge through an alluvial fan in the Atacama Desert, northern Chile: Mechanisms, magnitudes and causes, *Hydrol. Processes*, *16*(15), 3019–3035.

McCallum, A. M., M. S. Andersen, G. C. Rau, J. R. Larsen, and R. I. Acworth (2014), River-aquifer interactions in a semiarid environment investigated using point and reach measurements, *Water Resour. Res.*, *50*, 2815–2829, doi:10.1002/2012WR012922.

Moench, A. F., and C. C. Kisiel (1970), Application of the convolution relation to estimating recharge from an ephemeral stream, *Water Resour. Res.*, *6*(4), 1087–1094.

Nimmo, J. R., J. A. Deason, J. A. Izbicki, and P. Martin (2002), Evaluation of unsaturated zone water fluxes in heterogeneous alluvium at a Mojave Basin site, *Water Resour. Res.*, *38*(10), 1215, doi:10.1029/2001WR000735.

Pool, D. (2005), Variations in climate and ephemeral channel recharge in southeastern Arizona, United States, *Water Resour. Res.*, *41*, W11403, doi:10.1029/2004WR003255.

Rau, G. C., M. S. Andersen, A. M. McCallum, and R. I. Acworth (2010), Analytical methods that use natural heat as a tracer to quantify surface water–groundwater exchange, evaluated using field temperature records, *Hydrogeol. J.*, *18*(5), 1093–1110.

Rousseau-Gueutin, P., A. Love, G. Vasseur, N. Robinson, C. Simmons, and G. Marsily (2013), Time to reach near-steady state in large aquifers, *Water Resour. Res.*, *49*, 6893–6908, doi:10.1002/wrcr.20534.

Scanlon, B. R., K. E. Keese, A. L. Flint, L. E. Flint, C. B. Gaye, W. M. Edmunds, and I. Simmers (2006), Global synthesis of groundwater recharge in semiarid and arid regions, *Hydrol. Processes*, *20*(15), 3335–3370.

Shanafield, M., and P. G. Cook (2014), Transmission losses, infiltration and groundwater recharge through ephemeral and intermittent streambeds: A review of applied methods, *J. Hydrol.*, *511*, 518–529.

Shentsis, I., and E. Rosenthal (2003), Recharge of aquifers by flood events in an arid region, *Hydrol. Processes*, *17*(4), 695–712.

Simmers, I. (Ed.) (1997), *Recharge of Phreatic Qquifers in (Semi-) Arid Areas*, A. A. Balkema, Rotterdam, Netherlands.

Simmers, I. (2003), *Understanding Water in a Dry Environment: Hydrological Processes in Arid and Semi-Arid Zones*, A. A. Balkema, Lisse, Netherlands.

Taylor, R. G., B. Scanlon, P. Döll, M. Rodell, R. Van Beek, Y. Wada, L. Longuevergne, M. Leblanc, J. S. Famiglietti, and M. Edmunds (2013), Ground water and climate change, *Nat. Clim. Change*, *3*(4), 322–329.

Telvari, A., I. Cordery, and D. Pilgrim (1998), Relations between transmission losses and bed alluvium in an Australian arid zone stream, *Hydrol. Changing Environ.*, *2*, 361–366.

Theis, C. V. (1935), The relation between the lowering of the Piezometric surface and the rate and duration of discharge of a well using ground-water storage, *Eos Trans. AGU*, *16*(2), 519–524.

van Loon, A., and H. van Lanen (2013), Making the distinction between water scarcity and drought using an observation-modeling framework, *Water Resour. Res.*, *49*, 1483–1502, doi:10.1002/wrcr.20147.

Venetis, C. (1971), Estimating infiltration and/or the parameters of unconfined aquifers from ground water level observations, *J. Hydrol.*, *12*(2), 161–169.

Wheater, H. S., S. A. Mathias, and X. Li (2010), *Groundwater Modelling in Arid and Semi-Arid Areas*, Cambridge Univ. Press, Cambridge, U. K.